The Development of an Electroconductive SiC-ZrB_2 Ceramic Heater through Spark Plasma Sintering

Jin-Young Ju*, Cheol-Ho Kim*, Jae-Jin Kim*, Jung-Hoon Lee*, Hee-Seung Lee and Yong-Deok Shin†**

Abstract – The SiC-ZrB_2 composites were fabricated by combining 30, 35, 40 and 45vol.% of Zirconium Diboride (hereafter, ZrB_2) powders with Silicon Carbide (hereafter, SiC) matrix. The SiC-ZrB_2 composites, the sintered compacts, were produced through Spark Plasma Sintering (hereafter, SPS), and its physical, electrical, and mechanical properties were examined. Also, the thermal image analysis of the SiC-ZrB_2 composites was examined. Reactions between β-SiC and ZrB_2 were not observed via X-Ray Diffractometer (hereafter, XRD) analysis. The relative density of the SiC+30vol.%ZrB_2, SiC+35vol.%ZrB_2, SiC+40vol.%ZrB_2, and SiC+45vol.%ZrB_2 composites were 88.64%, 76.80%, 79.09% and 88.12%, respectively. The XRD phase analysis of the sintered compacts demonstrated high phase of SiC and ZrB_2 but low phase of ZrO_2. Among the SiC-ZrB_2 composites, the SiC+35vol.%ZrB_2 composite had the lowest flexural strength, 148.49MPa, and the SiC+40vol.%ZrB_2 composite had the highest flexural strength, 204.85MPa, at room temperature. The electrical resistivities of the SiC+30vol.%ZrB_2, SiC+35vol.%ZrB_2, SiC+40vol.%ZrB_2 and SiC+45vol.%ZrB_2 composites were 6.74×10^{-4}, 4.56×10^{-3}, 1.92×10^{-3}, and $4.95\times10^{-3}\Omega\cdot$cm at room temperature, respectively. The electrical resistivities of the SiC+30vol.%ZrB_2, SiC+35vol.%ZrB_2 SiC+40vol.%ZrB_2 and SiC+45[vol.%]ZrB_2 composites had Positive Temperature Coefficient Resistance (hereafter, PTCR) in the temperature range from 25℃ to 500℃. The V-I characteristics of the SiC+40vol.%ZrB_2 composite had a linear shape. Therefore, it is considered that the SiC+40vol.%ZrB_2 composite containing the most outstanding mechanical properties, high resistance temperature coefficient and PTCR characteristics among the sintered compacts can be used as an energy friendly ceramic heater or electrode material through SPS.

Keywords: Spark plasma sintering (SPS), positive temperature coefficient resistance (PTCR), V-I characteristics, thermal image, heater, and electrode material

1. Introduction

SiC, with its high melting point of 2,800℃, is a thermochemistrically stable IV-IV-compound semiconductor. In addition, based on its specific features, low thermal expansion coefficient, approximately 4.36×10^{-6}/℃ at 20-1,000℃, heating-conductivity, thermal impact resistivity, strength, and oxidation-resistance, SiC is considered an outstanding semiconductor [1]. However, due to the low efficiency of its diffusion caused by the strong covalent bond between Si and C, without sinter additives it is difficult to obtain sinter density. Also, below 1,000℃, the electrical resistivity of SiC is considered as Negative Temperature Coefficient Resistance (hereafter, NTCR), which causes increases in its temperature and uncontrollable electrical current in it, resulting in its overheating [2].

A transition metal boride, ZrB_2 generally has a high melting point of 3,200℃, high hardness, metal-like electric conduction, and high corrosion resistance against molded iron and slag. However, when it is employed as an electrical conduction material over 1,000℃, the lack of hardness and inside oxidation resistivity become a problem [3].

Hence, with the combination of SiC and ZrB_2, a SiC-ZrB_2 composite containing high electrical conductivity, superior oxidation resistance, and mechanical strength, which can be used as a conduction material or electrode at high and low temperature, can be obtained [4-6].

In general, a SiC ceramic has been produced via Hot Press (hereafter, HP), the solid-state sintering process, at approximately 1,950 ~ 2,100℃. And in order to lower HP's temperature below 1,950℃, the production method of the liquid-phase sintering process such as Al_2O_3+Y_2O_3 has been employed [7]. Compared to HP, SPS helps the surface of the molecular particle to access easier activation with the clarification of its surface. In addition, with high speed diffusion, highly efficient heating, fast sintering transformation, and the supply of high energy density, a high quality sintered compact at low temperature within a short

† Corresponding Author: School of Electrical and Information Engineering, Wonkwang Uni., Korea (ydshin@wonkwang.ac.kr).
* School of Electrical and Information Engineering, Wonkwang Uni., Korea (nympe1052@paran.com).
** Dept. of Electrical and Electronics, Kunjang College, Korea (hlee@kunjang.ac.kr).
Received : June 16, 2009; Accepted : August 31, 2009

time period can be obtained. Moreover, for various sintered compact materials such as metal and ceramics, it is possible to sinter them in a wide range of temperature and pressure, and it is also easy to control a sintered microstructure with no grain growth through SPS. Although HP is similar to SPS, significant differences of SPS from HP are that electric field is applied to both upper and lower electrodes, and materials are sintered within powders by direct heating only through SPS. However, according to many experimental studies, the density parameter of sintered compacts is still unclear, which results in a limitation in systematic examinations [8-11].

In this experiment, SPS was employed to obtain a ceramic composite of SiC-ZrB_2, a high density sintered compact at 1,500, 450~600℃ lower than HP's. In addition, in order to analyze the mechanical and electrical properties of the SiC-ZrB_2 composite through SPS, XRD, relative density, Scanning Electron Microscope (hereafter, SEM), Energy Dispersive Spectroscopy (hereafter, EDS), thermal image, V-I Characteristic, and the electrical resistivity of the SiC-ZrB_2 composite were examined. Based on these examinations, the SiC-ZrB_2 composite was diagnosed to determine whether it is useful as an energy friendly ceramic heater or electrode material.

2. Experimental Procedure

2.1 Compact Sintering

In this experiment, high-pure β-SiC (H. C. Starck, Germany, Grade BF12) and ZrB_2 (H. C. Starck, Germany, Grade B) were used as the starting materials. β-SiC and ZrB_2 were combined with the ratio of 70:30vol.%, 65:35vol.%, 60:40vol.%, and 55:45vol.%, and then they were designated as SZ30, SZ35, SZ40, and SZ45 in that order. Theses designated materials were combined with distilled water within the polyurethane bowl (volume: 1583.4 ㎖) containing acetone (approximately 500 ㎖). They were then applied to the planetary-ball-mill process with the two high purity SiC balls (10 ㎜ Φ, 20 ㎜ Φ) with 1:5 ratio of the number of SiC balls for 24 hours. After that, they were completely dehydrated for 12 hours at 100℃, and then the completely dehydrated materials, powders, were sieved by using a 60mesh screen.

2.2 SPS Process

After the dried powders were put in a graphite die with an inner diameter of 15㎜φ and enclosed with graphite foil, they were sintered using a Dr. Sinter SPS-515S apparatus (Sumitomo Coal Mining Co. Ltd., Tokyo, Japan) under the following conditions: 1,500℃, 10Pa vacuum and the uniaxial pressure of 30 MPa.

The sintering conditions were: (i) the powders were heated at high speed with 100℃/min up to the final sintering temperature of 1,500℃ for 5 minutes; (ii) a pressure of 30 MPa was constantly applied during the entire experiment; (iii) the on/off pulse sequence was 12:2, and after the sintering process was completed, the pressure was released, and then the electrical current was shut off. The final size of the SiC-ZrB_2 composites was approximately 15 mmΦ in diameter and 5 mmL in thickness.

2.3 Characterization Techniques

The theoretical densities of the SiC-ZrB_2 composites were calculated based on the rule of mixture (3.217g/㎤ for β-SiC, 6.085g/㎤ for ZrB_2), and the relative densities of the final SiC-ZrB_2 composites were measured based on the Archimedes method; each composite was measured 10 times. Phase identification of the SiC-ZrB_2 composites, the sintered compacts, was analyzed by XRD (D-Max 220V Rigaku, Japan) with CuKα radiation, and then element analysis was analyzed by EDS (Bruker Quantax 200, USA) connected to SEM. The final SiC-ZrB_2 composites, the sintered compacts, were ground by a diamond wheel, and the disks were machined to produce approximately 1.0-0.7-10 mm^3 dimension bars. The surfaces of the bars were then polished using 1 ㎛ diamond paste and were beveled at 45 degrees for mechanical testing (ASTM F394-78). The three-point flexural strength of each sintered compact was measured 5 times at room temperature; its outer span was 10 mm and its inner span was 8 mm (Instron, Model 4204, USA). After that, the microstructure of the sintered compacts, the fracture surface of each, was observed through SEM (XL30S Philips, USA). The sintered compacts were cut using wire-EDM (Electrical Discharge Machining) in order to produce machined pieces eventually to measure their electrical resistivity.

The electrical resistivity of each machined piece was measured 250 times between 25℃ to 500℃ [12] based on the Pauw method; the V-I characteristics of them naturally appeared. Lastly, 5 spots were randomly pointed on each machined piece, and they were measured using the thermal image camera (TVS-100E, Avio, Japan).

3. Experimental Results and Discussion

3.1 Relative Density

As demonstrated in Fig. 1, the relative densities of the sintered compacts (SZ30, SZ35, SZ40, and SZ45) were 88.64, 76.80, 79.09, and 88.12%, respectively. As the amount of ZrB_2 increased by 5vol.%, the porosities of SZ30, SZ35, SZ40, and SZ45 changed to 11.36, 23.20, 20.91, and 11.88%, respectively; SZ35 had the highest porosity and SZ30 had the lowest porosity.

According to the reaction equations shown in Table 1, condensed ZrO_2 phase, amorphous glass (the component for SiO_2 and B_2O_3), the formation of the vapor species of B_2O_3 (l,g), SiO(g), CO (g), and CO_2 (g) appeared [13-14].

However, as shown in Fig. 2, although the peak of condensed ZrO_2 appeared the same in all sintered compacts, the amorphous glass and the formation of the vapor species of SZ35 appeared stronger than that of SZ30. Based on the obtained result, it is considered that the relative density of SZ30 is higher than that of SZ35.

Based on the reaction equation 1 [13], the mass variation of SZ35 decreased by 3.1774%, the greatest decrease, causing the increased volume variation by 26.07%, which resulted in the lowest relative density of SZ35 as shown in Table 2.

According to the reaction equations, as SiC and ZrB_2 react with oxygen, all or some of the products, ZrO_2 (s), SiO_2 (s,l), B_2O_3(l,g), SiO(g), CO(g), and CO_2 (g), appeared [13-14].

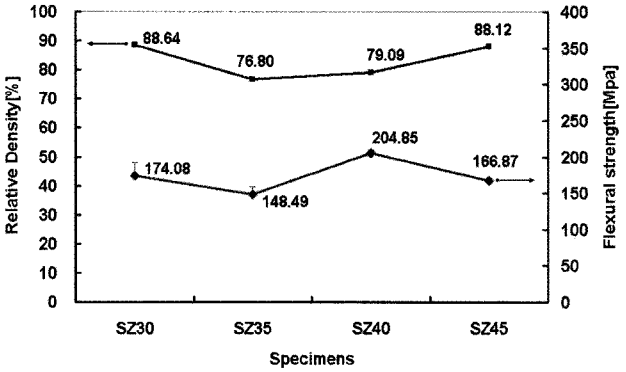

Fig. 1. Relative density and three-point flexural strength of the SiC-ZrB2 composites

Table 1. Reaction equations between starting materials (SiC, ZrB_2) and oxygen

Number of equation	Reaction Equations
1	$ZrB_2 + SiC + 4O_2(g) \rightarrow ZrO_2(s) + B_2O_3(g) + SiO_2(g) + CO(g)$
2	$SiC + \frac{3}{2}O_2 = SiO_2(s,l) + CO(g)$
3	$ZrB_2 + \frac{5}{2}O_2 = ZrO_2(s) + B_2O_3(l)$
4	$SiO_2 + CO = SiO(g) + CO_2(g)$
5	$B_2O_3(l) = B_2O_3(g)$

As demonstrated above, because the condensed phase and vapor species were formed, it is difficult to indicate the exact reaction speed of the measurement of mass change. In other words, due to the fact both mass increase and decrease occurred simultaneously, it is difficult to demonstrate the exact reaction speed [13].

Due to the fact that the volume variation of SZ45 (12.72%) increased by 1.0% compared to that of SZ30 (11.72%) whereas the mass variation of SZ45 (0.6754%) decreased by 0.2905% compared to that of SZ30 (0.9659%), the relative density of SZ45 appeared less than that of SZ30.

According to the reaction equations, as the reason for the mass variation of SZ30 being higher than that of SZ45, it is considered that the formation of the condensed ZrO_2 phase, B_2O_3 and SiO_2 are more preferable than that of SZ45.

Table 2. Mass and volume variation of the SiC-ZrB_2 composites

Specimen	mass before sintering[g]	mass after sintering[g]	mass variation[%]
SZ30	3.6028	3.568	▼ 0.9659
SZ35	3.7295	3.611	▼ 3.1774
SZ40	3.8562	3.814	▼ 1.0943
SZ45	3.9829	3.956	▼ 0.6754
Specimen	volume before sintering[cm^3]	volume after sintering[cm^3]	volume variation[%]
SZ30	0.8836	0.9872	▲ 11.72
SZ35	0.8836	1.1140	▲ 26.07
SZ40	0.8836	1.1050	▲ 25.05
SZ45	0.8836	0.9960	▲ 12.72

Table 3. EDS analysis of the SiC-ZrB2 composites

Specimen / Atom	SZ30	SZ35	SZ40	SZ45	Remarks
Si	23.03	26.06	21.58	37.42	atom%
Zr	4.79	5.21	5.96	13.56	
B	19.62	17.83	19.59	25.43	
C	43.39	40.04	40.09	19.17	
O	9.17	10.86	12.77	4.42	
Total	100.00	100.00	100.00	100.00	

3.2 Phase Analysis and Microstructure

As a result of the XRD analysis for the sintered compacts, SZ30, SZ35, SZ40 and SZ45, the peak of ZrO_2 appeared the same in all the sintered compacts demonstrated in Fig. 2.

It has been stated that the borosilicate glass layer, the component of SiO_2 and B_2O_3, is formed on the exposed surface of the sintered compacts to protect the oxidation of them [14].

As shown in Table 3, the amount of Si (37.42atom.%) of SZ45 appeared greater than that of Si (23.03atom.%) of SZ30. The reason for this result is considered to be that the borosilicate glass layer was formed better than the exposed surface of the ZrO_2 phase, according to the reaction equations in Table 1.

The microstructure, a fractured surface, of the sintered compact SZ30 observed through SEM reveals the lowest porosity (11.36%) as shown in Fig. 3.

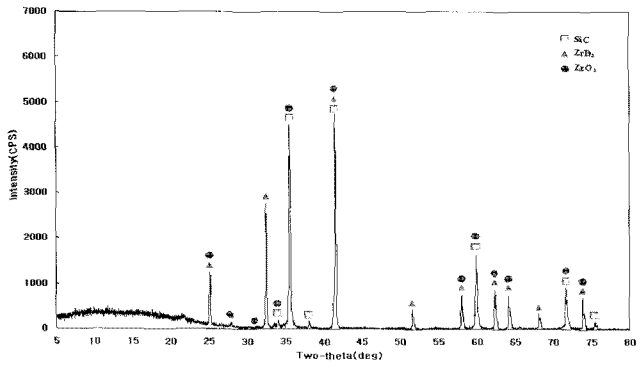

(a) SZ30

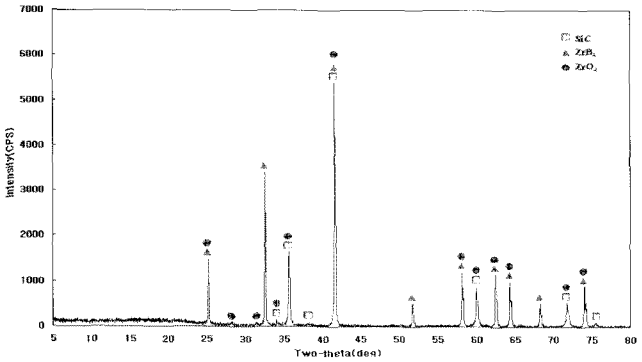

(b) SZ35

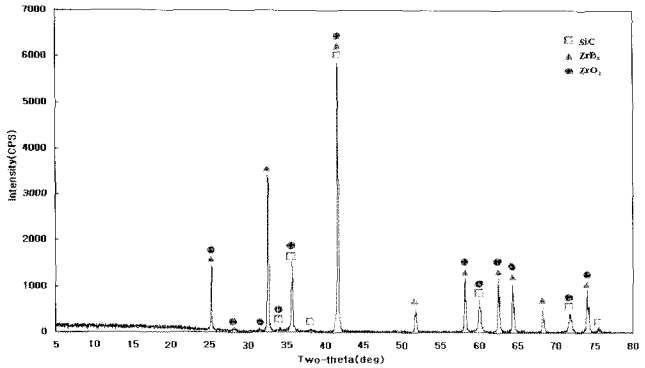

(c) SZ40

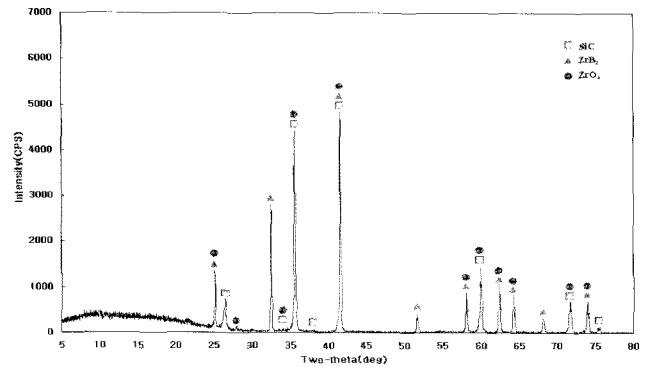

(d) SZ45

Fig. 2. X-ray diffraction analysis of the SiC-ZrB_2 composites

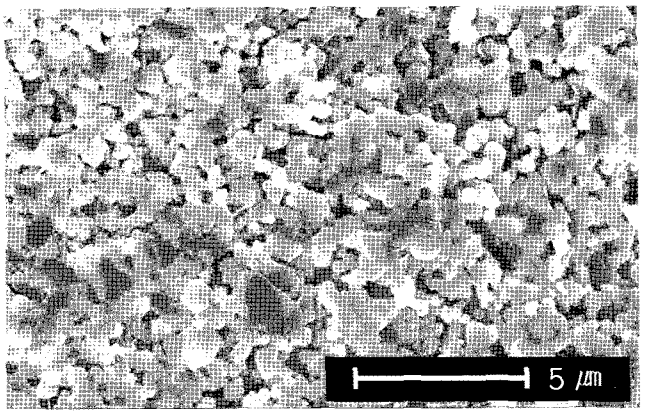

(a) SZ30

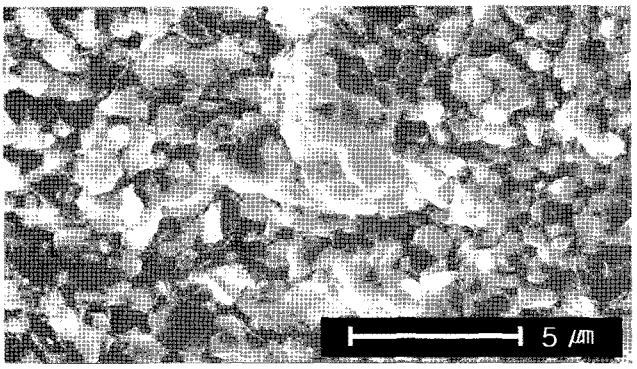

(b) SZ35

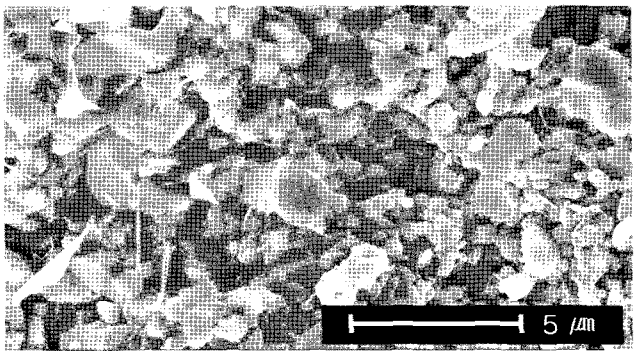

(c) SZ40

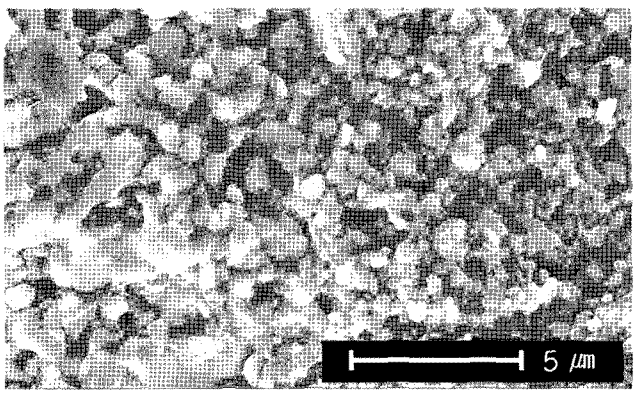

(d) SZ45

Fig. 3. SEM micrographs of the fracture surface of the SiC-ZrB_2 composites (×5000)

3.3 Mechanical Properties

The flexural strengths of the sintered compacts, 131.43 ~ 212.96MPa, at room temperature as shown in Fig. 1, were lower than that of SiC single crystal and ZrB_2 without porosity, 300~500MPa and 200~359MPa, respectively [15-18]. In general, the flexural strength is closely related to the grain growth of annealed ceramic. In addition, as ceramic microstructure becomes a coarse phase-shaped ceramic microstructure through ceramic annealing, the fracture toughness of the ceramic microstructure increases, but the flexural strength of it decreases [19-21]. However, with the second phase composition and proper annealing, the ceramic microstructure becomes more stable, and it can prevent decreases in flexural strength.

As demonstrated in Fig. 1, among the sintered compacts, SZ35 has the lowest flexural strength, 148.49Mpa. The reason for this is that during the sintering process the amount of the volatile component existed as porosity inside of the sintered compacts was the greatest at SZ35 [23.20%].

In addition, according to $\sigma_c=V_f\sigma_{SiC}+(1-V_f)\ \sigma_{ZrB2}$ (V_f is the volume variation of SiC), the reason for the flexural strength of SZ35, 148.49Mpa, lower than that of SZ35 of a SiC-ZrB_2 composite without porosity, 297.5~450.65Mpa, is considered as the effect of the transformation of porosity of grain boundaries. Also, the measured flexural strength of those were lower than that of SZ30 and SZ45 without porosity, 305~457.7MPa and 282.5~436.6MPa, respectively. The reason is that in ceramics the flexural strength is applied to the equation, $\sigma = \sigma_0\exp(-k\alpha)$ (σ_0 is the flexural strength of the material with no defect, α is residual porosity, and k is a constant) [22]. Therefore, flexural strength is highly dependent on the existence of porosity. However, it is difficult to accurately examine specific analysis regarding porosity due to the effects of grain growth, phase-shape, and grain boundary caused by annealing and debonding by the combination of liquid phase.

3.4 Electrical Resistivity

The electrical resistivity of SiC single crystal at room temperature was approximately 0.13Ω·cm. However, due to the NTCR characteristic, the resistivity dropped to 0.1Ω·cm up to 250℃, and when it reached 900℃ due to the PTCR characteristic, the resistivity increased to approximately 0.16Ω·cm.

The electrical resistivity of SiC polycrystalline was 0.1 ~ 0.3Ω·cm at room temperature. However, due to the NTCR characteristic, the resistivity dropped to one-third up to 800℃, and it gradually increased over 800℃ due to the PTCR characteristic.

The difference between SiC single crystal and polycrystalline comes from the fact that the grain of SiC polycrystalline is smaller than SiC single crystal and it also contains a greater amount of grain boundaries than SiC single crystal; grains in SiC polycrystalline grow as the sintering temperature increases up to 800℃, causing its electric resistivity to decrease [23].

The electrical conduction mechanism of SiC polycrystalline has been explained as the band model having electric potential barriers at grain boundaries. It has been stated that it goes over the electric potential barriers with the high thermal excitation at high temperature, and passes through the electric potential barriers with the tunnel and bulk conduction at low temperature [23].

As shown in Fig. 4, the electric resistivities of the sintered compacts, SZ30, SZ35, SZ40, and SZ45, were 6.74×10^{-4}, 4.56×10^{-3}, 1.92×10^{-3}, and 4.95×10^{-3}Ω·cm at room temperature, and 1.86×10^{-3}, 1.11×10^{-2}, 5.03×10^{-3}, 1.24×10^{-2}Ω·cm at 500℃, respectively. In addition, the resistance temperature coefficients of the sintered compacts were 3.706×10^{-3}/℃, 3.02×10^{-3}/℃, 3.41×10^{-3}/℃, and 3.17×10^{-3}/℃, in that order.

As demonstrated in Fig. 4, the electric resistivities of all sintered compacts has the PTCR characteristic because of the predominant flow of electric current along the chain formation of the ZrB_2 grain. The considerable reason for the electric resistivity of ZrB_2 which does not follow Vol.% dependence is that the condensed solid and porosity of volatile components affects the chain formation complicatedly.

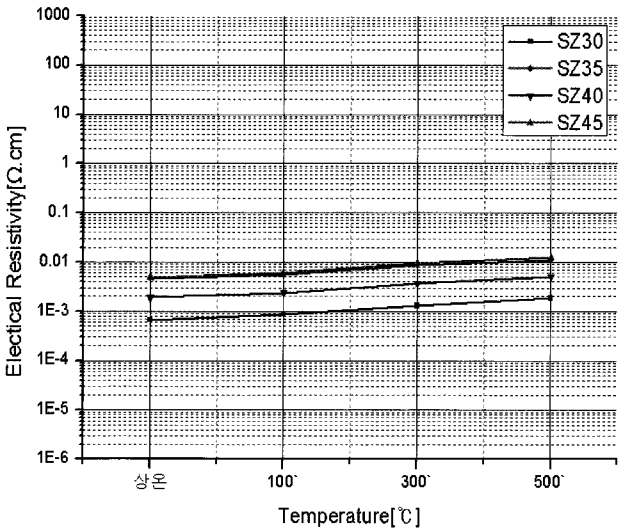

Fig. 4. Temperature dependence of electrical resistivities of the SiC-ZrB_2 composites

The electric resistivity of SZ40 at room temperature was 2.85 times greater than that of SZ30, and the electric resistance temperature coefficient (from room temperature to 500℃) of SZ40 was 0.92 time smaller than that of SZ30. The electric resistance temperature coefficient of SZ40 having the PTCR characteristic was slightly lower than that of SZ30, but its electric resistivity was slight higher and had outstanding mechanical characteristics. Therefore, it is considered that SZ40 sintered compact is most suitable to be used as a ceramic heater or electrode material.

3.5 V-I Characteristics and Thermal Images

As shown in Fig. 5, the V-I specific slopes of SZ30, SZ35, SZ40, and SZ45 were 2.72×10^{-2}, 1.63×10^{-1}, 7.07×10^{-2}, and 1.79×10^{-1} at room temperature, and 7.07×10^{-2}, 3.97×10^{-1}, 1.83×10^{-1}, and 4.52×10^{-1} at 500℃.

The V-I characteristics of all SiC-ZrB_2 composites were shown as a linear shape except SZ35 at 500℃ which was shown as an irregular shape as seen in Fig. 5. As a result, they can be used as an electrode material of Ohmic contact, except the one case.

As shown in Fig. 6, 3[A] was applied to the sintered compacts. The temperature points at the start and after 1 minute were measured as shown in Table 4, respectively. The increasing temperature deviation of SZ30 and SZ40 were 0.99℃ and 0.32℃, respectively, whereas that of SZ35 and SZ45 didn't appear. After 1 minute, the points of the average increasing temperature of SZ30, SZ35, SZ40, and SZ45 were 5.92, 11.80, 8.88, and 13.36℃, respectively. This result occurred because the SiC-ZrB_2 composite is a resistance thermal material dependent on electric resistivity. Each point of the average increasing temperature of SZ45 was 13.36℃, which is 7.44℃ higher than that of SZ30.

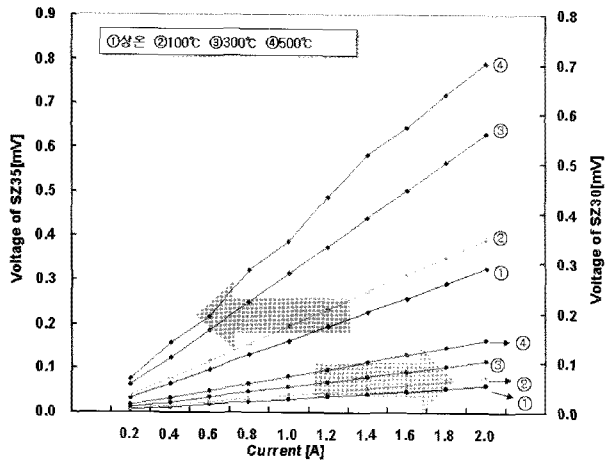

(a) SZ30 and SZ35

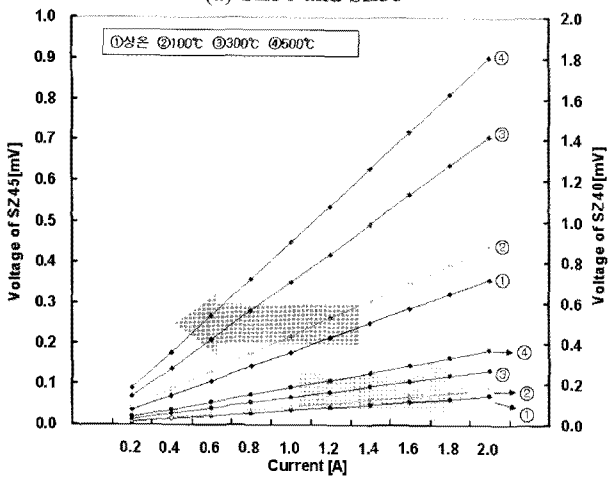

(b) SZ40 and SZ45

Fig. 5. V-I characteristics of the SiC-ZrB2 composites

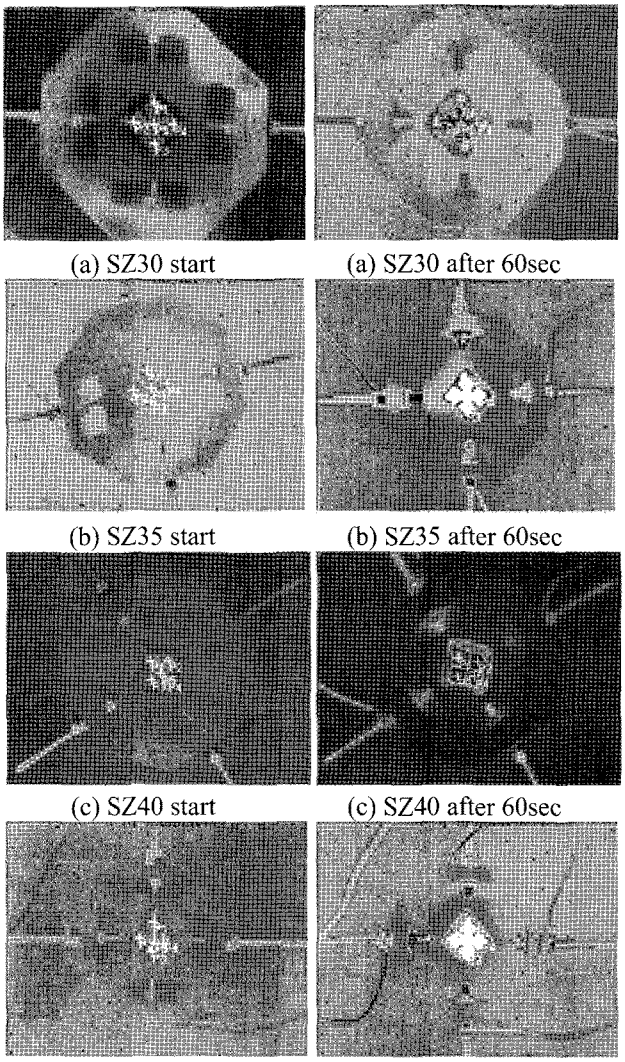

(a) SZ30 start (a) SZ30 after 60sec

(b) SZ35 start (b) SZ35 after 60sec

(c) SZ40 start (c) SZ40 after 60sec

(d) SZ45 start (d) SZ45 after 60sec

Fig. 6. Thermal images of the SiC-ZrB2 composites

Table 4. Point temperature of the SiC-ZrB2 composites

Specimen	SZ30		SZ35	
Time(sec) / point[℃]	Start	60	Start	60
P1	23.70	29.46	23.41	35.19
P2	23.70	30.27	23.32	35.19
P3	23.61	29.28	23.32	35.19
P4	23.70	29.28	23.41	35.19
P5	23.61	29.64	23.51	35.19
Specimen	**SZ40**		**SZ45**	
Time(sec) / point[℃]	Start	60	Start	60
P1	24.75	33.41	21.78	35.19
P2	24.37	33.45	21.87	35.19
P3	24.46	33.22	21.87	35.19
P4	24.37	33.54	21.87	35.19
P5	24.28	33.51	21.78	35.19

4. Conclusion

The characteristics of the SiC-ZrB_2 composites, the sintered compacts, produced by combining β-SiC with 30vol.% of ZrB_2 increased by 5vol.% of it through SPS are as follows:

1. The changes of the porosity of the sintered compacts were 11.36, 23.20, 20.91, and 11.88%, respectively. The relative density of the SiC+30vol.%ZrB_2 composite was the highest, 88.64%, and that of the SiC+35vol.%ZrB_2 composite was the lowest, 76.80%.

2. There was no reaction between the SiC and ZrB_2, but ZrB_2 existed as the second phase.

3. The flexural strength of the SiC+35vol.%ZrB_2 composite was the weakest, 148.49MPa, and that of the SiC+40vol.%ZrB_2 composite was strongest, 204.85MPa.

4. The electrical resistivities of SZ30, SZ35, SZ40, and SZ45 were 6.74×10^{-4}, 4.56×10^{-3}, 1.92×10^{-3}, and 4.95×10^{-3}Ω·cm at room temperature, and 1.86×10^{-3}, 1.11×10^{-2}, 5.03×10^{-3}, and 1.24×10^{-2}Ω·cm at 500℃, respectively.

5. The resistance temperature coefficient of SZ30, SZ35, SZ40, and SZ45 were 3.706×10^{-3}/℃, 3.02×10^{-3}/℃, 3.41×10^{-3}/℃, and 3.17×10^{-3}/℃, containing the PTCR characteristic.

6. With the V-1 characteristic of the SiC-ZrB_2 composites, except SZ35 at 500℃, indicating a linear shape, they can be used as an electrode material of Ohmic contact.

7. The points of average increasing temperature deviation of the SiC+30vol.%ZrB_2 and SiC+40vol.%ZrB_2 composites were 0.99℃ and 0.32℃, whereas that of the SiC+35vol.%ZrB_2 and SiC+45vol.%ZrB_2 composites didn't appear. After 1 minute, the point of average increasing temperature of the SiC+40vol.%ZrB_2 composite was 8.88℃, which is 2.96℃higher than that of the SiC+30vol.%ZrB_2 composite.

In conclusion, it is considered that the most suitable condition to develop an energy friendly ceramic heater or electrode material of the SiC-ZrB_2 composite through SPS, among the sintered compacts, is to apply the SiC+40vol.%ZrB_2 composite containing the most outstanding mechanical properties, high resistance temperature coefficient, and PTCR characteristics.

Acknowledgements

This paper was supported by wonkwang university in 2009

References

[1] Patricia A. Hoffman, "Thermo Elastic Properties of Silicon Carbide-Titanium Diboride Particulate Composites," *M. S Thesis*, Pennslyvania State University, 1992.

[2] Hideto Hashiguchi, and Hisashi Kimugasa, "Electrical Resistivity of α-SiC Ceramics Added with NiO," *J. Ceram. Soc. Japan*, 102[2], pp. 160-164, 1994.

[3] M. Nakamura, I Shigematsu, K. Kanayama, and Y. Hirai, "Surface Damage in ZrB2-based Composite Ceramics Induced by Electro-Discharge Machining," *J. Mater. Sci.*, 26, pp. 6078-6082, 1991.

[4] Y. D. Shin, and J. Y. Ju, "Effect of In Situ YAG on Microstructure and Properties of the Pressureless-Sintered SiC-ZrB_2 Electroconductive Ceramic Composites," *Trans. KIEE*, vol. 55C, no. 11, pp. 505-513, 2006.

[5] Y. D. Shin, and J. Y. Ju, "Effect of Annealing Temperature on Microstructure and Properties of the Pressureless-Sintered SiC-ZrB_2 Electroconductive Ceramic Composites," *Trans. KIEE*, vol. 55C, no. 9, pp. 434-441, 2006.

[6] Y. D. Shin, J. Y. Ju, and T. H. Ko, "Effects of Boride on Microstructure and Properties of the Electroconductive Ceramic Composites of Liquid-Sintered Silicon Carbide System," *Trans. KIEE*, vol. 56C, Nn. 9, pp. 1602-1608, 2007.

[7] Yong-Deok Shin, and Jing-Young Ju, "Properties and Manufacture of the β-SiC-ZrB_2 Composites Densified by Liquid-Phase Sintering," *Trans. KIEE*. vol. 48C, no. 2, pp. 93-97, 1998.

[8] K. A. Khor, L. G. Yu, S. H. Chan, and X. J. Chen, "Densification of plasma sprayed YSZ electrolytes by spark plasma sintering (SPS)," *Journal of the European Ceramic Society*, 23 1855-1863, 2003.

[9] Xiaoyan Song, Xuemei Liu, and Jiuxing Zhang, "Neck Formation and Self-Adjusting Mechanism of Neck Growth of Conducting Powders in Spark Plasma Sintering," *J. Am. Ceram. Soc.*, 89 [2] 494–500, 2006.

[10] Shu-Qi Guo, Toshiyuki Nishimura, Yutaka Kagawa, and Jenn-Ming Yang, "Spark Plasma Sintering of Zirconium Diborides," *J. Am. Ceram. Soc.*, 91 [9], 2848–2855, 2008.

[11] Zhijian Shen, Mats Johnsson, Zhe Zhao, and Mats Nygren, "Spark Plasma Sintering of Alumina," *J. Am. Ceram. Soc.*, 85 [8] 1921–27, 2002.

[12] L. J. van der Paw, "A Method of Measuring Specific Resistivity and Hall Effect of Discs of Arbitrary Shape," *Philips Res. Repts.* 13, 1-9, 1958.

[13] Alireza Rezaie, William G. Fahrenholtz, and Gregory E. Hilmas, "Oxidation of Zirconium Diboride-Silicon Carbide at 1500℃ at a Low Partial Pressure of Oxygen," *J. Am. Ceram. Soc.*, 89 [10], pp. 3240-3245, 2006.

[14] F. Monteverde, and A. Bellosi, "Oxidation of ZrB_2-Based Ceramics in Dry Air," *Journal of The Electrochemical Society.*, 150 [11], B552-B559, 2003.

[15] Diletta Sciti, Cesare Melandri, and Alida Bellosi, "Properties of ZrB_2-Reinforced Tenary Composites,"

Advanced Engineering Materials, 6 [9], pp. 775-781, 2004.
[16] Cathleen Mroz, "Zirconium Diboride," *J. Am. Ceram. Soc.*, Bull., 74 [6], pp. 164-165, 1995.
[17] F. Monteverde, A. Bellosi, and S. Guicciardi, "Processing and Properties of Zirconium Diboride-based Composites," *Journal of the European Ceramic Society*, 22. pp. 279-288, 2002.
[18] J. B. Hurst, and S. Dutta, "Simple Processing Method for High-strength Silicon Carbide," *J. Am. Ceram. Soc.*, 70 [11], pp. C303-308, 1987.
[19] M. Nader, F. Aldinger, and M. J. Hoffmann, "Influence of the α/β Phase Transformation on Microstructural Development and Mechanical Properties of Liquid Phase Sintered Silicon Carbide," *J. Mat. Sci.*, 34. pp. 1197-1204, 1999.
[20] Y. W. Kim, M. Mitomo, H. Emoto, and J. G. Lee, "Effect of Initial α-Phase Content on Microstructure and Mechanical Properties of Sintered Silicon Carbidea," *J. Am. Ceram. Soc.*, 81 [12], pp. 3136-3140, 1998.
[21] Y. W. Kim, M. Mitomo, and H. Hirotsuru, "Microstructure Development of Silicon Carbide Containing Large Seed Grains," *J. Am. Ceram. Soc.*, 80 [1], pp. 99-105, 1997.
[22] Weimin Wang, Zhengyi Fu, Hao Wang, and Runzhang Yuan, "Influence of Hot Pressing Sintering Temperature and Time on Microstructure and Mechanical Properties of TiB_2 Ceramics," *Journal of the European Ceramic Society*, 22. pp. 1045-1049, 2002.
[23] Akira Kondo, "Electrical Conduction Mechanism in Recrystallized SiC," *Journal of the Ceramic Society of Japan. Int. Edition*, vol. 100, pp. 1204-1208, 1993.

Jin-Young Ju was born in Korea in 1974. He graduated in 1997 from Wonkwang University, Iksan, Korea, where he received his M.S. and Ph.D. degrees in electrical engineering in 1999 and 2009, respectively. He worked at the technology research institute of Hanbo NISCO as a researcher. At present, he is working in the research institute at Balsan Industry and is also a professor at Wonkwang University.

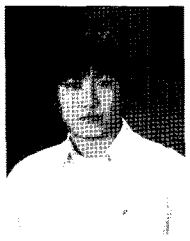

Cheol-Ho Kim was born in Korea in 1982. He graduated from the School of Electrical Electronics and Information Engineering from Wonkwang University, Iksan, Korea, in 2009. Presently, he is studying his Master's degree at Wonkwang University.

Jae-Jin Kim was born in Korea in 1974. He graduated from the Department of Electrical Engineering at Wonkwang University, Iksan, Korea, in 2001. Presently, he is studying for his Master's degree at Wonkwang University and is working at KESCO.

Jung-Hoon Lee was born in Korea in 1983. He graduated from the School of Electrical Electronics and Information Engineering at Wonkwang University, Iksan, Korea, in 2008. Presently, he is studying his Master's degree at Wonkwang University.

Hee-Seung Lee was born in Korea in 1964. He received his B.S. and M.S. degrees in Electrical Engineering from Wonkwang University, Iksan, Korea, in 1990 and 1992, respectively. Presently, he is on a Doctor's course at Wonkwang University and is a Professor at Kunjang College, Kunsan, Korea.

Yong-Deok Shin was born in Korea in 1953. He received his B.S. degree in Electrical Engineering from Wonkwang University, Iksan, Korea, in 1983, where he worked as a research assistant and part time lecturer from 1983 to 1988. He worked at the Center Research Institute of Keyang Electric Machinery Co., Ltd. from 1988 to 1990. He received his Ph.D. degree from Sungkyunkwan University, Seoul, Korea, in 1991. He was a visiting Professor at Pennsylvania State University, Pennsylvania, USA, in 1998 and 2005, respectively. Presently, he is Professor of the School of Electrical and Information Engineering at Wonkwang University, Iksan, Korea. He is a fellow member of the Korean Institute of Electrical Engineers (KIEE).